

CRYSTAL STRUCTURE OF METAL-ORGANIC FRAMEWORKS OBTAINED FROM A HETEROMETALLIC PIVALATE COMPLEX $[\text{Li}_2\text{Zn}_2(\text{py})_2(\text{piv})_6]$

A. A. Sapianik^{1,2*}, E. R. Dudko^{1,2},
D. G. Samsonenko^{1,2}, and V. P. Fedin^{1,2}

In the interaction of the heterometallic complex $[\text{Li}_2\text{Zn}_2(\text{py})_2(\text{piv})_6]$ (piv^- is the pivalate anion, py is pyridine) with 2,5-dibromoterephthalic acid ($\text{H}_2\text{Br}_2\text{-bdc}$) or 9,10-anthracenedicarboxylic acid (H_2adc), two coordination polymers $[\text{Li}(\text{DMF})(\text{HBr}_2\text{-bdc})]$ (**1**) and $(\text{Me}_2\text{NH}_2)[\text{Zn}(\text{Hadc})(\text{adc})]\cdot\text{DMF}\cdot\text{H}_2\text{O}$ (**2**) are obtained. During the synthesis, the initial tetranuclear heterometallic fragment is completely fragmentated. When the same complex interacts with nitroterephthalic acid ($\text{H}_2\text{NO}_2\text{-bdc}$), a heterometallic metal-organic framework $(\text{Me}_2\text{NH}_2)[\text{LiZn}(\text{NO}_2\text{-bdc})_2]\cdot\text{DMF}$ (**3**) is formed. Resulting coordination polymer **3** has a three-dimensional porous structure; binuclear heterometallic carboxylate moieties $\{\text{LiZn}(\text{COO})_3\}$ act as secondary building blocks.

DOI: 10.1134/S0022476620120148

Keywords: lithium, zinc, heterometallic complexes, coordination polymers, polycarboxylic acids, X-ray diffraction analysis.

INTRODUCTION

The chemistry of metal-organic frameworks (MOFs) has been developed more and more rapidly. Publications on the first compounds that can be related to MOFs appeared about thirty years ago [1,2], and the works that gave impetus to the development of this field appeared twenty years ago [3,4]. This class of compounds continues to attract more and more attention owing to the widest range of applications [5-7]: gas adsorption and separation [8-10], catalysis [11], sensors [12,13], and magnetic devices [14]. Heterometallic MOFs take a special place because of a combination of properties inherent in different metal cations; these compounds have unique functionalities. Nonetheless, it is often nontrivial to obtain heterometallic MOFs [15]. The application of pre-synthesized heterometallic complexes as sources of secondary building blocks enables a more rational synthesis of MOFs because it is often difficult to obtain these compounds from a mixture of salts of respective metals.

In this work, to synthesize new MOFs a pivalate complex of the composition $[\text{Li}_2\text{Zn}_2(\text{py})_2(\text{piv})_6]$ was used [16] as a source of metal centers. Three new MOFs were obtained: $[\text{Li}(\text{DMF})(\text{HBr}_2\text{-bdc})]$ (**1**), $(\text{Me}_2\text{NH}_2)[\text{Zn}(\text{Hadc})(\text{adc})]\cdot\text{DMF}\cdot\text{H}_2\text{O}$ (**2**),

¹Nikolaev Institute of Inorganic Chemistry, Siberian Branch, Russian Academy of Sciences, Novosibirsk, Russia;
*sapianik@niic.nsc.ru. ²Novosibirsk State University, Novosibirsk, Russia. Original article submitted May 18, 2020; revised May 18, 2020; accepted May 21, 2020.

$(\text{Me}_2\text{NH}_2)[\text{LiZn}(\text{NO}_2\text{-bdc})_2]\cdot\text{DMF}$ (**3**). In the first two cases, the heterometallic moiety is completely decomposed, and MOF **3** contains a binuclear heterometallic $\{\text{LiZn}(\text{COO})_3\}$ fragment. The composition and structure of compounds **1-3** are determined by single crystal X-ray diffraction (XRD).

EXPERIMENTAL

Precursors and solvents (acetonitrile >99%, N,N-dimethylformamide (DMF), 2,5-dibromoterephthalic acid ($\text{H}_2\text{Br}_2\text{-bdc}$), 9,10-anthracene dicarboxylic acid (H_2adc), nitroterephthalic acid ($\text{H}_2\text{NO}_2\text{-bdc}$)) were no worse than chemically pure grade (Fig. 1) and used without additional purification. The pivalate complex $[\text{Li}_2\text{Zn}_2(\text{py})_2(\text{piv})_6]$ was prepared by the previously described procedure [16]. The elemental analysis was carried out in the Analytical Laboratory, Institute of Inorganic Chemistry, Siberian Branch, Russian Academy of Sciences, Novosibirsk on a Vario Micro Cube CHNS-analyzer. Powder XRD data were collected on a Shimadzu XRD 7000S diffractometer (CuK_α radiation).

Synthesis of $[\text{Li}(\text{DMF})(\text{HBr}_2\text{-bdc})]$ (1**)**. To a solution of $[\text{Li}_2\text{Zn}_2(\text{py})_2(\text{piv})_6]$ (25 mg, 0.03 mmol) in DMF (0.5 mL) a solution of $\text{H}_2\text{Br}_2\text{-bdc}$ (57 mg, 0.18 mmol) in DMF (0.5 mL) was added. The total volume of the reaction mixture was brought to 5 mL with acetonitrile. The mixture was placed in a sealed glass ampoule, heated to 130 °C with a heating rate of 1 °C/min, and then left at 130 °C for 48 h. Rectangular, elongated colorless crystals formed were used to solve the structure by synchrotron single crystal XRD. The crystals obtained is the only solid-phase reaction product and the synthesis is reproduced with the yield of ~50%.

Synthesis of $(\text{Me}_2\text{NH}_2)[\text{Zn}(\text{Hadc})(\text{adc})]\cdot\text{DMF}\cdot\text{H}_2\text{O}$ (2**)**. To a solution of $[\text{Li}_2\text{Zn}_2(\text{py})_2(\text{piv})_6]$ (25 mg, 0.03 mmol) in DMF (0.5 mL) a solution of H_2adc (48 mg, 0.18 mmol) in DMF (0.5 mL) was added. The total volume of the reaction mixture was brought to 5 mL with acetonitrile. The mixture was placed in a sealed glass ampoule, heated to 130 °C with a heating rate of 1 °C/min, and then left at 130 °C for 24 h. Beige rectangular crystals formed were used to solve the structure by synchrotron single crystal XRD. The crystals obtained is the only solid-phase reaction product and the synthesis is reproduced with a high yield of ~70%.

Synthesis of $(\text{Me}_2\text{NH}_2)[\text{LiZn}(\text{NO}_2\text{-bdc})_2]\cdot\text{DMF}$ (3**)**. To a $[\text{Li}_2\text{Zn}_2(\text{py})_2(\text{piv})_6]$ sample (25 mg, 0.03 mmol) dissolved in DMF (0.5 mL) 0.5 mL of a $\text{H}_2\text{NO}_2\text{-bdc}$ solution in DMF (37 mg, 0.18 mmol) was added, and the solution volume was brought to 5 mL with acetonitrile. Then the reaction mixture was thermostated at 130 °C for 24 h. Beige rectangular crystals formed were used for single crystal XRD. The synthesis is well reproduced with a high yield of ~60%. Found (%): C 41.6, H 3.4, N 9.1. $\text{C}_{21}\text{H}_{21}\text{LiN}_4\text{O}_{13}\text{Zn}$. Calculated (%): C 41.4, H 3.5, N 9.2.

Single crystal XRD study. XRD data for single crystals of **1** and **2** were collected at 100 K on the BELOK beamline ($\lambda = 0.79272 \text{ \AA}$ and 0.79313 \AA , j -scanning with a step of 1.0), National Research Center “Kurchatov Institute” using a Rayonix SX165 CCD detector ($\lambda = 0.79272 \text{ \AA}$ and 0.79313 \AA , φ -scanning with a step of 1.0°). Integration, absorption correction, determination of unit cell parameters were performed using the *XDS* program package [17].

Single crystal XRD data for **3** were measured at 200 K on an automated Agilent Xcalibur diffractometer equipped with an AtlasS2 area detector (graphite monochromator, $\lambda(\text{MoK}_\alpha) = 0.71073 \text{ \AA}$, ω -scanning with a step of 0.5°). Integration, absorption correction, determination of unit cell parameters were performed using the *CrysAlisPro* software [18]. The

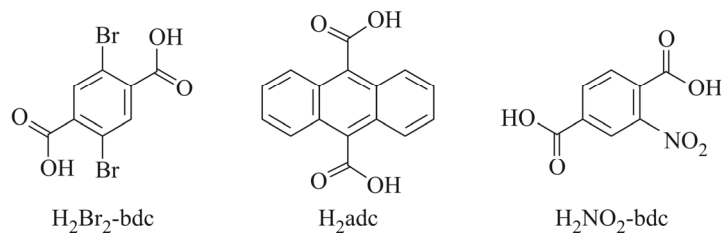


Fig. 1. Organic ligands used for the synthesis of MOFs.

TABLE 1. Crystallographic Characteristics and Parameters of the Diffraction Experiment

Parameter	1	2	3
Chemical formula	C ₁₁ H ₁₀ Br ₂ LiNO ₅	C ₃₈ H ₃₆ N ₂ O ₁₀ Zn	C ₂₁ H ₂₁ LiN ₄ O ₁₃ Zn
<i>M</i> , g/mol	402.96	746.06	609.73
Crystal system	Monoclinic	Monoclinic	Monoclinic
Space group	<i>P</i> 2 ₁ / <i>c</i>	<i>P</i> 2 ₁ / <i>n</i>	<i>Cc</i>
<i>a</i> , <i>b</i> , <i>c</i> , Å	9.0120(18), 17.930(3), 8.613(4)	9.4860(17), 22.0840(7), 16.3990(7)	8.7719(4), 17.3337(8), 18.1755(12)
β, deg	93.29(5)	91.716(5)	101.207(6)
<i>V</i> , Å ³	1389.4(7)	3433.9(6)	2710.9(3)
<i>Z</i>	4	4	4
<i>D</i> _{calc} , g/cm ³	1.926	1.443	1.494
μ, mm ⁻¹	7.646	1.041	0.976
<i>F</i> (000)	784	1552	1248
Crystal dimensions, mm	0.10×0.05×0.03	0.10×0.06×0.05	0.22×0.19×0.15
θ scanning range, deg	2.534-28.522	1.727-30.991	2.285-29.036
<i>h</i> , <i>k</i> , <i>l</i> index range	-10 ≤ <i>h</i> ≤ 7, -21 ≤ <i>k</i> ≤ 21, -9 ≤ <i>l</i> ≤ 10	-6 ≤ <i>h</i> ≤ 12, -28 ≤ <i>k</i> ≤ 28, -16 ≤ <i>l</i> ≤ 21	-11 ≤ <i>h</i> ≤ 9, -23 ≤ <i>k</i> ≤ 16, -18 ≤ <i>l</i> ≤ 24
<i>N</i> _{hkl} measured / unique	6039 / 2426	13757 / 6999	7258 / 4324
<i>R</i> _{int}	0.0696	0.0412	0.0240
<i>N</i> _{hkl} and <i>I</i> > 2σ(<i>I</i>)	2079	5450	4161
GOOF on <i>F</i> ²	1.074	1.095	1.076
<i>R</i> factors (<i>I</i> > 2σ(<i>I</i>))	<i>R</i> ₁ = 0.0737, <i>wR</i> ₂ = 0.2008	<i>R</i> ₁ = 0.0644, <i>wR</i> ₂ = 0.1887	<i>R</i> ₁ = 0.0400, <i>wR</i> ₂ = 0.1075
<i>R</i> factors (over all reflections)	<i>R</i> ₁ = 0.0829, <i>wR</i> ₂ = 0.2057	<i>R</i> ₁ = 0.0781, <i>wR</i> ₂ = 0.1993	<i>R</i> ₁ = 0.0419, <i>wR</i> ₂ = 0.1094
Residual el. density (max / min), e/Å ³	2.236 / -1.020	1.174 / -0.693	0.651 / -0.466

structures were solved using the SHELXT program [19] and refined with the full-matrix least-squares technique in the anisotropic (except for hydrogen atoms) approximation using the SHELXL program [20]. Positions of hydrogen atoms of organic ligands are calculated geometrically and refined with a riding model. Crystallographic data and refinement details for the structures are listed in Table 1. Complete tables of interatomic distances and bond angles, atomic coordinates and displacement parameters for structures **1-3** have been deposited with the Cambridge Crystallography Data Center (CCDC 2003486-2003488) and also can be received from the authors.

RESULTS AND DISCUSSION

A series of isoreticular MOFs previously obtained based on [Li₂Zn₂(py)₂(piv)₆] [Li₂Zn₂(bpy)(R-bdc)₃] (where R is a substituent in the benzene ring of the terephthalate anion bdc²⁻, bpy is 4,4'-bipyridyl) contains in their composition the initial tetranuclear {Li₂Zn₂} fragment with complete replacement of both pivalate anions by terephthalate ones with different substituents in the benzene ring and pyridine by bridging dipyridyl [16]. MOFs of this series are unique examples from the standpoint of using pre-synthesized heterometallic complexes and as precursors of materials with variable functional properties. The application of diverse R in the terephthalate linker can provide fine variation of the structure and functionalization of channels in the structure. In this work, we used three different analogues of terephthalic acid:

2,5-dibromoterephthalic ($\text{H}_2\text{Br}_2\text{-bdc}$), 9,10-anthracene dicarboxylic (H_2adc), and nitroterephthalic ($\text{H}_2\text{NO}_2\text{-bdc}$) acids. At the first stage, the reaction mixture also contained 4,4'-bipyridyl because it is one of two structure-forming linkers in the series $[\text{Li}_2\text{Zn}_2(\text{bpy})(\text{R-bdc})_3]$. However, since it is not contained in the structure of obtained compounds **1-3**, the synthesis of these coordination polymers was further optimized and performed without this ligand. The synthesis was performed under solvothermal conditions in a sealed ampoule in a mixture of DMF–acetonitrile solutions. The composition and structure of MOFs were determined by single crystal XRD.

In the synthesis of MOF **1**, the initial heterometallic $\{\text{Li}_2\text{Zn}_2\}$ moiety is completely decomposed, which seems to be due to the increased acidity of dibromoterephthalic acid relative to its unsubstituted analogue. Longer heating at a high temperature also plays a certain role, which facilitates the decomposition of the initial complex. The structure of $[\text{Li}(\text{Br}_2\text{-Hbdc})(\text{DMF})]$ compound (**1**) contains lithium cations as metal centers. This cation is in a distorted tetrahedral environment of four oxygen atoms: three oxygen atoms belong to three carboxyl groups of three different hydrodibromoterephthalate anions, and the fourth oxygen atom belongs to the coordinated molecule of the DMF solvent (Fig. 2a). Four neighboring cations are linked by hydrodibromoterephthalate anions into layers with the **sql** topology (Fig. 2b). Two structurally independent layers are packed as ABAB (Fig. 2c). The structure is dense, cavities capable of accommodating any additional guest molecules are absent in them. The Li–O distances are in the range 1.887(15)–1.957(14) Å.

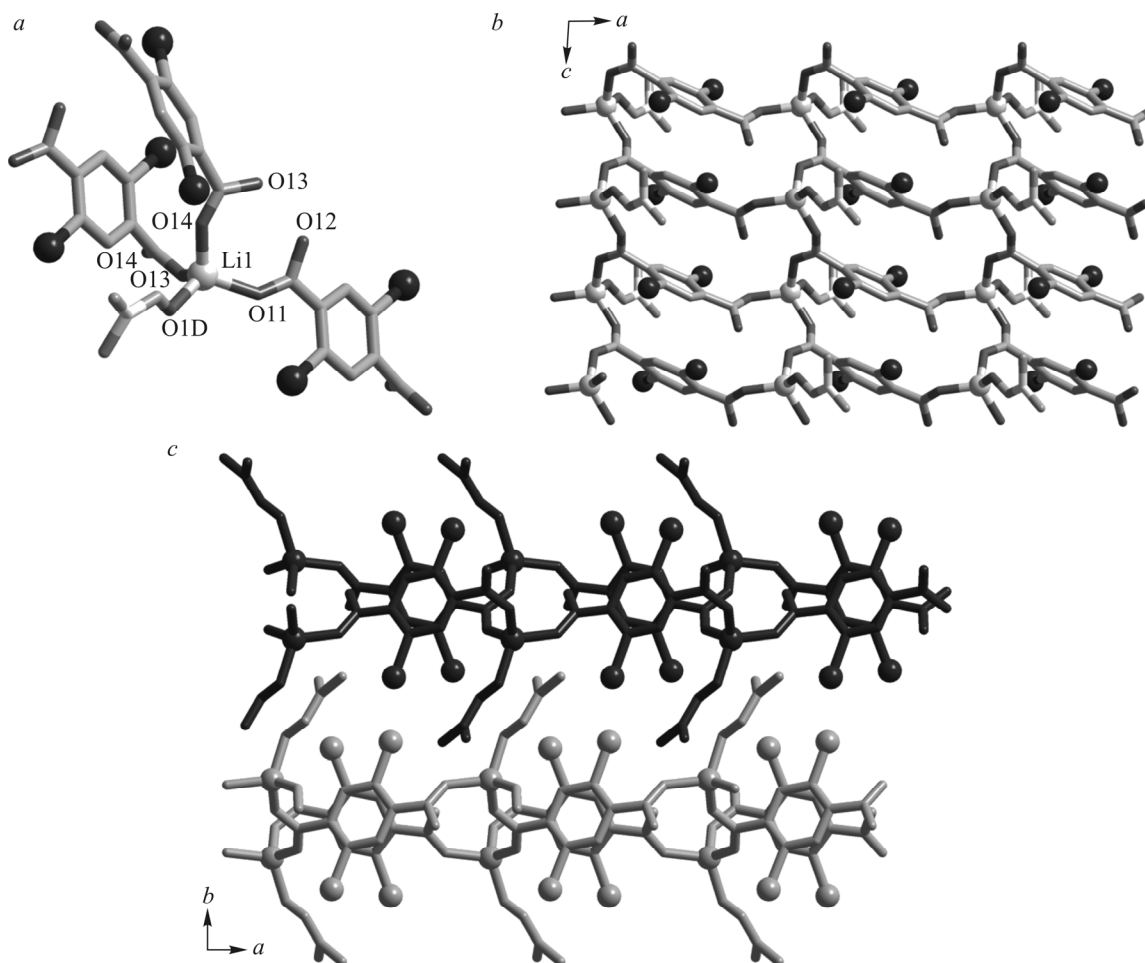


Fig. 2. Coordination environment of a lithium cation in **1** (*a*); structure of the layer in the *ac* plane, lithium atoms are shown by light gray balls, nitrogen atoms are shown by gray, carbon atoms are shown by darker gray, oxygen atoms are shown by dark gray, bromine atoms are shown by black (*b*); the arrangement of layers relative to each other (*c*). Hydrogen atoms are omitted.

In a reaction with another structural analogue of terephthalic acid (anthracene dicarboxylic acid), the initial heterometallic $\{\text{Li}_2\text{Zn}_2\}$ fragment is also completely decomposed. In structure **2** formed, the metal center is the zinc cation in a strongly distorted octahedral environment. The metal atom coordinates two oxygen atoms from two different anthracene dicarboxylates and one oxygen atom from two partially protonated anthracene dicarboxylates (Fig. 3a). The Zn–O distances are within the range 1.967(2)–1.982(2) Å. As a result, a three-dimensional anionic framework is formed: $(\text{Me}_2\text{NH}_2)[\text{Zn}(\text{Hadc})(\text{adc})]\cdot\text{DMF}\cdot\text{H}_2\text{O}$ (**2**). An interesting feature is the intergrowth of the structure (Fig. 3b). Thus, one unit cell contains two independent frameworks. Nonetheless, the structure remains sufficiently porous. The rest of the free space contains dimethylammonium cations and guest DMF and water molecules. Dimethylammonium cations are found structurally from single crystal XRD data and are hydrogen bonded with a free oxygen atom of the carboxyl group of anthracene dicarboxylate anion. Water and DMF molecules are also stabilized by hydrogen bonds at a certain position in the structure; they occupy 17% of the free space remained in the structure (Fig. 3c); positions of these molecules are also found from direct single crystal XRD data.

By the reaction of nitroterephthalic acid with the pivalate complex $[\text{Li}_2\text{Zn}_2(\text{py})_2(\text{piv})_6]$ in the presence of 4,4'-bipyridyl, we have previously obtained one of the frameworks of the $[\text{Li}_2\text{Zn}_2(\text{bpy})(\text{R}-\text{bdc})_3]$ series [16] and we obtained single crystals of another compound (**3**), when the concentration of 4,4'-bipyridyl decreased. Later, having excluded 4,4'-bipyridyl from the reaction mixture and varying the ratios of initial reagents and the temperature, we managed to optimize the synthesis and steadily produce single crystals of $(\text{Me}_2\text{NH}_2)[\text{LiZn}(\text{NO}_2-\text{bdc})_2]\cdot\text{DMF}$ compound (**3**) with a good yield. During the reaction, the initial heterometallic $\{\text{Li}_2\text{Zn}_2\}$ moiety is partially fragmented to binuclear $\{\text{LiZn}\}$, this being likely to be caused by a sufficiently high synthesis temperature. This fragmentation was exemplified in some other reactions described in our works [21–23]. In the structure of **3**, zinc and lithium cations are disordered over two positions. Every Li/Zn cation is in a distorted tetrahedral environment of four carboxyl oxygen atoms of four different nitroterephthalate anions (Fig. 4a). The structure contains two types of nitroterephthalate anions (Fig. 4b). In the first, both carboxyl groups bridge two Li/Zn cations inside the secondary building unit $\{\text{LiZn}(\text{COO})_3\}$ (Fig. 4b), thus, anions of the first acid provide the structure growth only in the *bc* plane (Fig. 5). Anions of the second acid differ in that only one carboxyl group links two Li/Zn cations inside the $\{\text{LiZn}(\text{COO})_3\}$ unit, whereas the second carboxyl group links two Li/Zn cations from two different $\{\text{LiZn}(\text{COO})_3\}$ units (Fig. 4b), as a result of which the structure grows perpendicular to the *bc* plane (Fig. 5). Finally, a three-dimensional structure with an intricate intergrown topology is formed. The structure contains a system of connected channels filled with

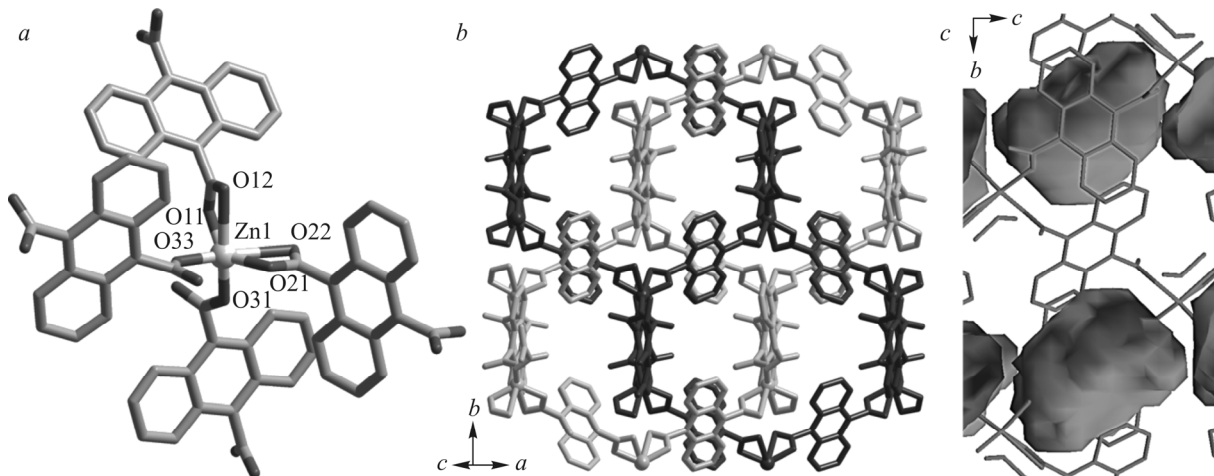


Fig. 3. Coordination environment of a zinc cation in **2** (a); projection of the structure with two independent networks (b); cavities filled with guest molecules in **2** (c). Zinc atoms are shown by light gray balls, carbon atoms are shown by light gray, oxygen atoms are shown by dark gray. Hydrogen atoms are omitted.

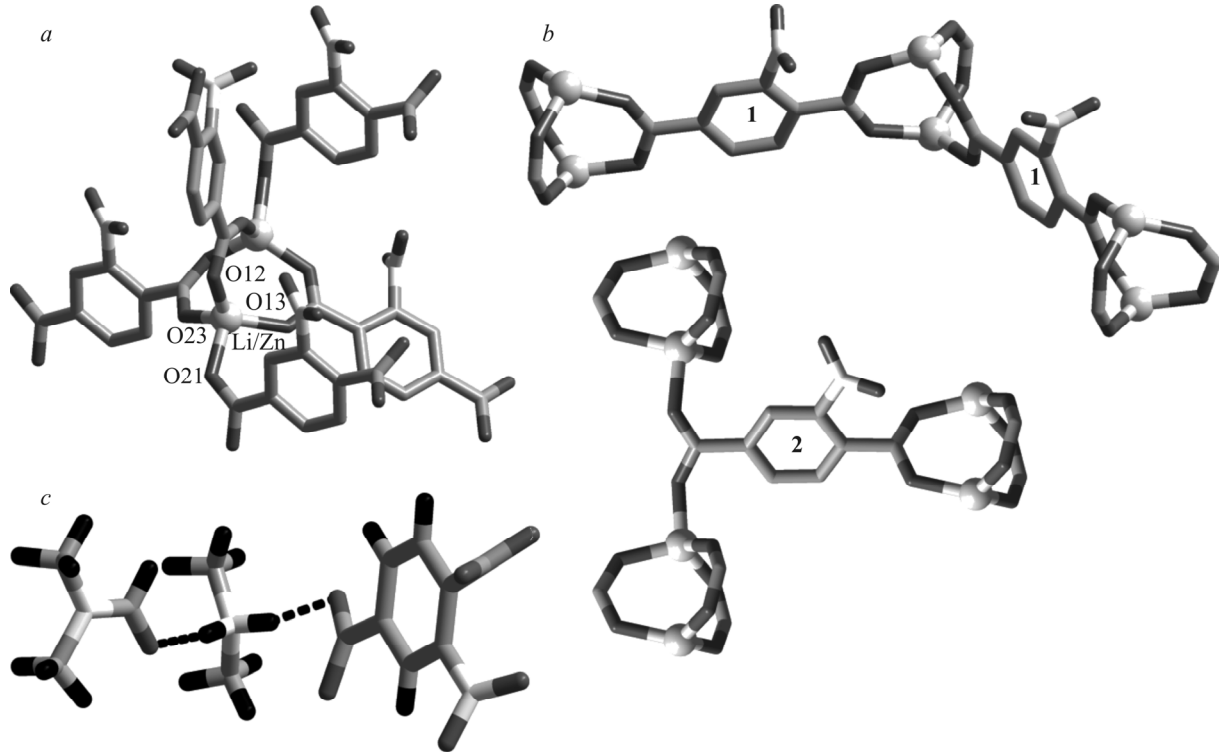


Fig. 4. Structure of the secondary building unit in **3** and the coordination environment of the Li/Zn cation (*a*); the coordination of carboxyl groups of acid anions of types **1** and **2** (*b*); hydrogen bonds between the framework and the dimethylammonium cation (*c*). Li/Zn atoms are shown by light gray balls, nitrogen atoms are shown by gray, carbon atoms are shown by darker gray, oxygen atoms are shown by dark gray, and hydrogen atoms are shown by black.

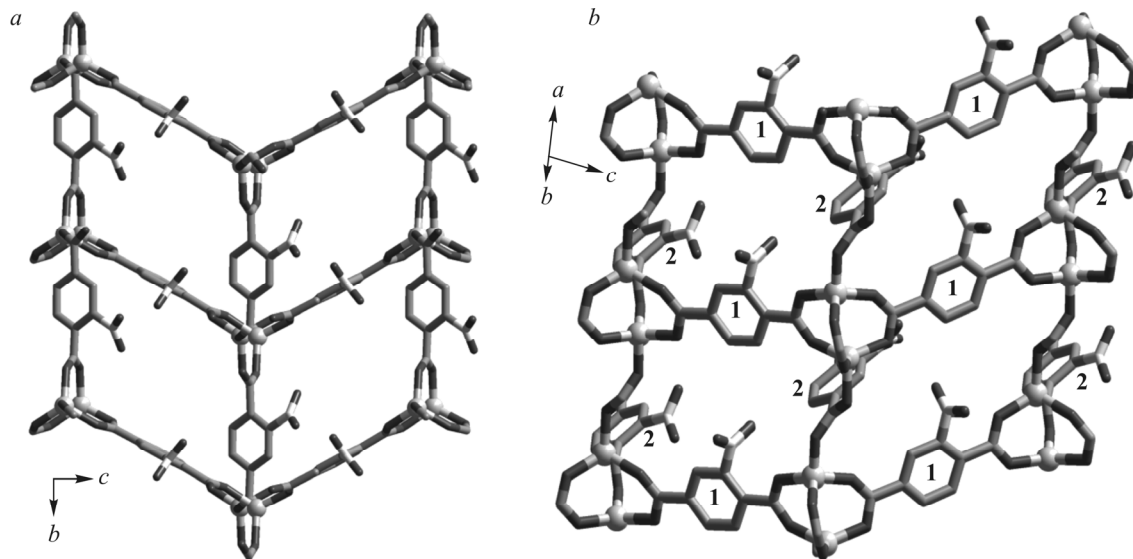


Fig. 5. Projections of the structure of **3** in the *bc* plane (*a*); detailed arrangement and structure growth due to the acid anions of types **1** and **2** (*b*).

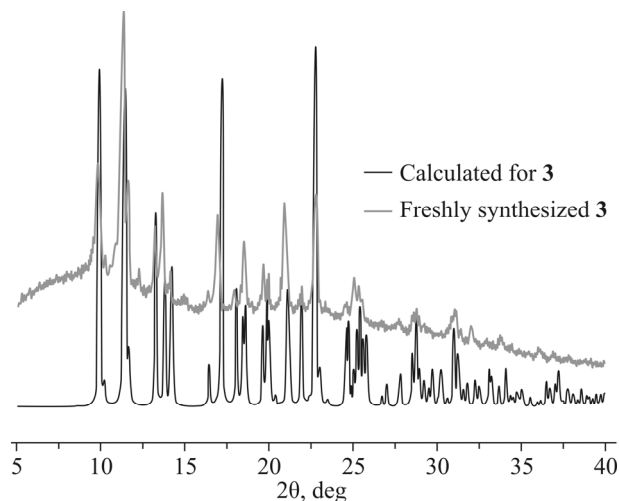


Fig. 6. Comparison of the experimental and calculated powder XRD patterns of compound 3.

dimethylammonium cations and guest DMF molecules. As in the case of compound **2**, all positions of cations and guest molecules were found from direct single crystal XRD data. Thus, a dimethylammonium cation is bound by weak hydrogen bonds made by hydrogen atoms with oxygen atoms of the nitroterephthalate anion and DMF molecules (Fig. 4c). The Li/Zn–O distances are within 1.886(4)–1.971(3) Å. Powder XRD data confirm the phase purity of the sample obtained (Fig. 6), and elemental analysis data are well consistent with the structural formula determined by single crystal XRD.

Despite that we failed to obtain direct structural analogues of a series $[\text{Li}_2\text{Zn}_2(\text{bpy})(\text{R}-\text{bdc})_3]$, the application of similar conditions made it possible to synthesize three new MOFs. MOF **2** ($(\text{Me}_2\text{NH}_2)[\text{Zn}(\text{Hadc})(\text{adc})]\cdot\text{DMF}\cdot\text{H}_2\text{O}$) is a promising porous framework based on a polyaromatic ligand, which is needed to study the luminescent properties of the framework itself and inclusion compounds. MOF **3** ($(\text{Me}_2\text{NH}_2)[\text{LiZn}(\text{NO}_2-\text{bdc})_2]\cdot\text{DMF}$) is also a three-dimensional framework whose structure has a system of channels. Moreover, this coordination polymer is one of the examples of heterometallic MOFs.

CONCLUSIONS

In this work, we obtained and structurally characterized three new MOFs: $[\text{Li}(\text{DMF})(\text{HBr}_2-\text{bdc})]$ (**1**), $(\text{Me}_2\text{NH}_2)[\text{Zn}(\text{Hadc})(\text{adc})]\cdot\text{DMF}\cdot\text{H}_2\text{O}$ (**2**), $(\text{Me}_2\text{NH}_2)[\text{LiZn}(\text{NO}_2-\text{bdc})_2]\cdot\text{DMF}$ (**3**). They are formed by the interaction of heterometallic carboxylate complex $[\text{Li}_2\text{Zn}_2(\text{py})_2(\text{piv})_6]$ with different dicarboxylic acids on heating. The composition and structure of compounds obtained in the reactions are determined by single crystal XRD. In the reactions studied, the structure of the initial heterometallic fragment is not always maintained. During the synthesis of **1** and **2**, the initial heterometallic fragment is completely decomposed, and complexes containing only one type of metals are formed. In the structure of MOF **3**, a binuclear tricarboxylate fragment $\{\text{LiZn}\}$ is retained. MOFs **2** and **3** obtained are of special interest from the standpoint of studying the luminescent properties due to the presence of aromatic ligands, including conjugated, and the sorption properties due to the three-dimensional highly bound structure in which channels are present.

ACKNOWLEDGMENTS

The authors are grateful to P. V. Dorovatskii and V. A. Lazarenko for assisting in the synchrotron single crystal XRD experiment with compounds **1** and **2**.

FUNDING

The study was supported by the Russian Science Foundation (project No. 19-73-00171).

CONFLICT OF INTERESTS

The authors declare that they have no conflict of interests.

REFERENCES

1. B. F. Hoskins and R. Robson. *J. Am. Chem. Soc.*, **1989**, *111*, 5962.
2. B. F. Hoskins and R. Robson. *J. Am. Chem. Soc.*, **1990**, *112*, 1546.
3. M. Kondo, T. Yoshitomi, K. Seki, H. Matsuzaka, and S. Kitagawa. *Angew. Chem., Int. Ed.*, **1997**, *36*, 1725.
4. H. Li, M. Eddaoudi, M. O'Keeffe, and O. M. Yaghi. *Nature*, **1999**, *402*, 276.
5. S. Yuan, L. Feng, K. Wang, J. Pang, M. Bosch, C. Lollar, Y. Sun, J. Qin, X. Yang, P. Zhang, Q. Wang, L. Zou, Y. Zhang, L. Zhang, Y. Fang, J. Li, and H.-C. Zhou. *Adv. Mater.*, **2018**, *30*, 170430.
6. S. L. Griffin and N. R. Champness. *Coord. Chem. Rev.*, **2020**, *414*, 213295.
7. M. O. Barsukova, S. A. Sapchenko, D. N. Dybtsev, and V. P. Fedin. *Russ. Chem. Rev.*, **2018**, *87*, 1139.
8. K. Sumida, D. L. Rogow, J. A. Mason, T. M. McDonald, E. D. Bloch, Z. R. Herm, T.-H. Bae, and J. R. Long. *Chem. Rev.*, **2012**, *112*, 724.
9. M. P. Suh, H. J. Park, T. K. Prasad, and D.-W. Lim. *Chem. Rev.*, **2012**, *112*, 782.
10. Y. He, W. Zhou, G. Qian, and B. Chen. *Chem. Soc. Rev.*, **2014**, *43*, 5657.
11. H. Konnerth, B. M. Matsagar, S. S. Chen, M. H. G. Precht, F.-K. Shieh, and K. C.-W. Wu. *Coord. Chem. Rev.*, **2020**, *416*, 213319.
12. H. Kau, S. Sundriyal, V. Pachauri, S. Ingebrandt, K.-H. Kim, A. L. Sharma, and A. Deep. *Coord. Chem. Rev.*, **2019**, *401*, 213077.
13. L. Chen, D. Liu, J. Peng, Q. Du, and H. He. *Coord. Chem. Rev.*, **2020**, *404*, 213113.
14. G. Mínguez Espallargas and E. Coronado. *Chem. Soc. Rev.*, **2018**, *47*, 533.
15. A. A. Sapianik and V. P. Fedin. *Russ. J. Coord. Chem.*, **2020**, *46*, 443–457.
16. A. A. Sapianik, E. N. Zorina-Tikhonova, M. A. Kiskin, D. G. Samsonenko, K. A. Kovalenko, A. A. Sidorov, I. L. Eremenko, D. N. Dybtsev, A. J. Blake, S. P. Argent, M. Schröder, and V. P. Fedin. *Inorg. Chem.*, **2017**, *56*, 1599.
17. W. Kabsch. *Acta Crystallogr., Sect. D*, **2010**, *66*, 125.
18. CrysAlisPro. V. 1.171.39.46. Rigaku Oxford Diffraction, **2018**.
19. G. M. Sheldrick. *Acta Crystallogr., Sect. A*, **2015**, *71*, 3.
20. G. M. Sheldrick. *Acta Crystallogr., Sect. C*, **2015**, *71*, 3.
21. A. A. Sapianik, E. E. Semenenko, D. G. Samsonenko, D. N. Dybtsev, and V. P. Fedin. *J. Struct. Chem.*, **2018**, *59*, 487.
22. A. A. Sapianik, M. A. Kiskin, D. G. Samsonenko, A. A. Ryadun, D. N. Dybtsev, and V. P. Fedin. *Polyhedron*, **2018**, *145*, 147.
23. A. A. Sapianik, M. A. Kiskin, K. A. Kovalenko, D. G. Samsonenko, D. N. Dybtsev, N. Audebrand, Y. Sun, and V. P. Fedin, *Dalton Trans.*, **2019**, *48*, 3676.